

Parameterization of subgrid scale energy injection in oceanic flows

Meelis J. Zidikheri¹

Jorgen S. Frederiksen²

(Received 8 August 2008; revised 10 November 2008)

Abstract

Dissipative terms are usually employed to parameterize subgrid fluxes of energy and enstrophy in turbulent flows. However, in certain flows, such as oceanic flows, when the dissipation is calculated self-consistently it turns out to be negative and hence numerically unstable. A solution to this problem is offered in this study in the form of a stochastic subgrid scale parametrization scheme. It is a spectral scheme employing matrices that generalize the classical eddy dissipation and stochastic forcing variance to include vertical transfers. Using a baroclinic model with typical oceanic parameters the scheme is able to maintain the resolved-scale spectra exceptionally well when the energy injection scale is in the subgrid scales. This work has implications for ocean climate modelling where the resolution is typically too coarse to resolve the energy injection due to baroclinic instability.

<http://anziamj.austms.org.au/ojs/index.php/ANZIAMJ/article/view/1404>

gives this article, © Austral. Mathematical Soc. 2008. Published December 1, 2008. ISSN 1446-8735. (Print two pages per sheet of paper.)

Contents

1	Introduction	C460
2	The baroclinic model	C462
3	Subgrid scale parameterizations	C464
4	Model results	C466
5	Discussion and Conclusion	C471
	References	C472

1 Introduction

Direct Numerical Simulations (DNSs) of turbulent flows require that the smallest scales of motion be resolved due to the non-linear coupling between different scales of motion. Unfortunately, the range of scales excited can be vast for high Reynolds number flows. For example, in the atmosphere and oceans, the range of scales can be 10^7 – 10^{-2} m. This presents a formidable computational challenge. A solution to this problem is to perform simulations at manageable resolutions, and to parameterize the interactions with the subgrid scales in some fashion. These simulations are called Large Eddy Simulations (LESs). Practically all climatic simulations with general circulation models of the ocean and atmosphere fall into this category.

Large scale oceanic and atmospheric flows are quasi two dimensional flows. In the inviscid limit, two dimensional flows possess two quadratic invariants, namely, energy and enstrophy. The phenomenology of two dimensional turbulence predicts that enstrophy injected at some intermediate scale is cascaded towards smaller scales (higher wavenumbers) while energy is cas-

caded towards the large scales (lower wavenumbers). The classical subgrid-scale parameterization scheme employs the so-called eddy viscosity and its variants. In atmospheric and oceanic modelling, this commonly takes the form of a hyperviscosity, which is a very scale selective damping term that removes enstrophy near the truncation scale.

However, as shown by Leith [1] and Kraichnan [2], there is a problem with this approach when it is used in quasi two dimensional flows. Because of the dual cascade, the eddy viscosity should actually be negative at the large and intermediate scales. This represents an injection of energy from the subgrid scales. Furthermore, the approaches above have the deficiency of being deterministic. Such formulations capture the average energy transfer between the resolved and subgrid scales but do not capture the stochastic nature of this interaction. Hence, deterministic formulations tend to overestimate the predictability of the flow. This view is consistent with statistical closure theories. In these formulations, the subgrid tendency can be written as a combination of linear deterministic and noise terms, as demonstrated by Frederiksen and Davies for quasi two dimensional atmospheric flows [3].

In the atmospheric context, deterministic eddy viscosity formulations may appear to be sufficient in many situations, such as in climate studies. However, in the oceanic context the situation is quite different. Because the oceanic radius of deformation is only about 50 km, the scale of energy injection (due to baroclinic instability) is unresolved in oceanic circulation models. From the barotropic (depth independent) point of view, the subgrid scales act as a source of energy, due to the inverse cascade process of two dimensional turbulence, and the net dissipation may be negative. From the stratified (two layer) turbulence point of view [4], there are two vertical modes: barotropic (vertical average) and baroclinic (vertical shear). The barotropic part of the flow receives energy from the subgrid scales while the baroclinic part of the flow sends energy to the subgrid scales. Hence a dissipative term might be appropriate for the baroclinic part of flow, but not the barotropic part.

If one were to pursue the deterministic eddy viscosity approach consis-

tently in low resolution oceanic flows, then one has to define a negative eddy viscosity. However, this is numerically unstable. In contrast, within a stochastic formulation, the energy injection occurs via a random forcing term, which is combined with a damping term, leading to a simulation that is usually numerically stable. The methodology that we employ was articulated and used by Frederiksen and Kepert [5] in the context of atmospheric barotropic flows. It is a stochastic method that uses DNS to calculate the statistics of the flow, and is thus easily applicable to a variety of flows. Frederiksen and Kepert showed that the calculated damping parameter (drain eddy dissipation) and the variance of the random forcing (stochastic backscatter) are similar to those calculated from closure theories [3]. In the two level (baroclinic) case, the scalar parameters are generalized to 2×2 matrices at each wavenumber to account for correlation in the vertical [6].

2 The baroclinic model

The two level quasi-geostrophic potential vorticity (QGPV) equations form the so-called Baroclinic Model. When relaxed towards a mean zonal shear, they generate exponentially growing modes (baroclinic instability) peaked at a wavenumber somewhat larger than the deformation scale, which is around 50 km for the ocean. The spectral form of these equations is

$$\frac{\partial \mathbf{q}_{mn}^j}{\partial t} = i \sum_{pq} \sum_{rs} A_{nqs}^{mpr} \zeta_{-pq}^j \mathbf{q}_{-rs}^j - D_0^j(\mathbf{m}, \mathbf{n}) \zeta_{mn}^j + \kappa \left(\tilde{\mathbf{q}}_{mn}^j - \mathbf{q}_{mn}^j \right), \quad (1)$$

where $j = 1, 2$ correspond to upper and lower levels, respectively; \mathbf{m} and \mathbf{n} are zonal and total wavenumbers, respectively; the field that is stepped forward in time $\mathbf{q}_{mn}^j = \zeta_{mn}^j - (-1)^j F_L[\mathbf{n}(\mathbf{n} + 1)]^{-1} (\zeta_{mn}^1 - \zeta_{mn}^2)$ is the potential vorticity wave amplitude; ζ_{mn}^i is the vorticity; and the generalized complex operator $D_0^j = \alpha^j + \nu^j [\mathbf{n}(\mathbf{n} + 1)]^\rho - B \text{im}[\mathbf{n}(\mathbf{n} + 1)]^{-1}$ describes both dissipation and the frequency of Rossby waves if $B \neq 0$. On the sphere, $B = 2$;

however, for the results presented here we set $\mathbf{B} = \mathbf{0}$ to maintain the vertical symmetry of the flow. F_L is the layer coupling parameter. $\tilde{\mathbf{q}}_{mn}^j$ is the value towards which \mathbf{q}_{mn}^j is being relaxed on a timescale given by κ^{-1} ; it is a representation of (Equator-Pole) differential heating effects. The interaction coefficients $\mathbf{A}_{nqs}^{mpr} = -\mathbf{K}_{nqs}^{mpr}/[\mathbf{q}(\mathbf{q} + 1)]$, with \mathbf{K}_{nqs}^{mpr} explicitly given by Frederiksen and Kepert [5], describe the non-linear coupling between the streamfunction and vorticity. The numerical integration of the model is described by Bourke et al. [7].

In this study, the following parameters have been chosen to reproduce spectra typical of the oceans. The drag, α^j , has been set to a damping time of 20 days for both layers; the hyperviscosity $\nu^j = 1.68 \times 10^8 \text{ m}^4 \text{ s}^{-1}$ for both layers; the order of the Laplacian (in physical space) operator $\rho = 2$. The zonal current is relaxed towards $\tilde{\mathbf{u}}^j = \tilde{\mathbf{U}}^j \cos \phi$, where ϕ is the latitude, and $\tilde{\mathbf{U}}^j$ are the maximum currents (at the equator), implying that only the solid body rotation mode with $(\mathbf{m}, \mathbf{n}) = (0, 1)$ is relaxed; the maximum zonal currents are $\tilde{\mathbf{U}}^1 = 0.1875 \text{ ms}^{-1}$ and $\tilde{\mathbf{U}}^2 = -0.1875 \text{ ms}^{-1}$; the relaxation time, κ^{-1} , is 1.16 days. The layer coupling constant, $F_L = 2.4 \times 10^{-10} \text{ m}^{-2}$, corresponds to a deformation radius of about 50 km. The resolution corresponds to triangular truncation at wavenumber 252 (T252) with 768×384 grid points. The model is integrated to statistical steady state and then further stepped forward in time for 104 days. With this choice of parameters, and by setting $\mathbf{B} = \mathbf{0}$, the kinetic energy is equally distributed across the two layers. Such a flow was considered by Salmon [4], and coined *Equivalent Layers*. The motivation for considering equivalent layers is the high degree of symmetry, which aids understanding and simplifies the presentation of the results. Figure 1(a) shows the obtained kinetic and potential energy spectra. Figure 1(b) shows the corresponding spectra in the barotropic-baroclinic (BTBC) formulation where the barotropic vorticity is defined as $\zeta_{mn}^+ = \frac{1}{2} (\zeta_{mn}^1 + \zeta_{mn}^2)$ and the baroclinic vorticity as $\zeta_{mn}^- = \frac{1}{2} (\zeta_{mn}^1 - \zeta_{mn}^2)$. The kinetic energy peak is seen to be dominated by barotropic kinetic energy. This barotropic energy at the large scales is a result of an inverse cascade of energy from the injection scales ($\mathbf{n} \approx 100$). Hence, commonly used climate model truncations corre-

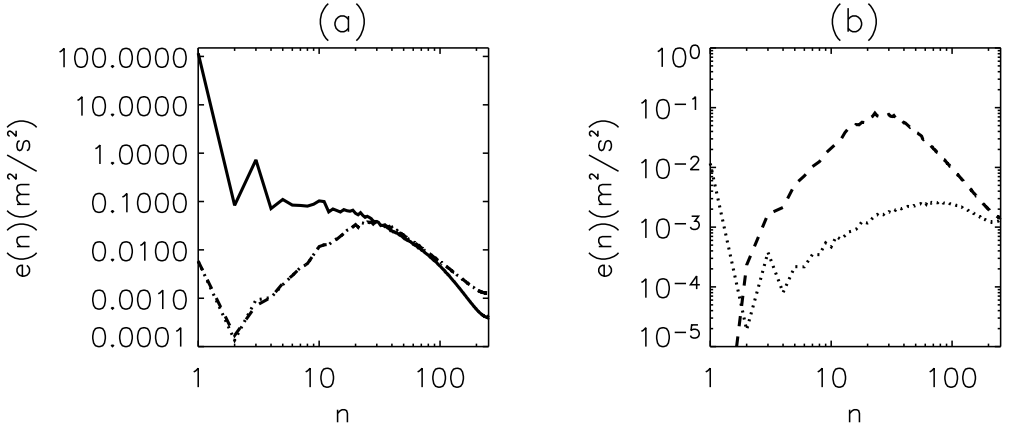


FIGURE 1: Energy spectra as functions of total wavenumber: (a) potential energy (solid), Level 1 kinetic energy (dashed), and Level 2 kinetic energy (dotted); (b) barotropic kinetic energy (dashed) and baroclinic kinetic energy (dotted).

sponding to wavenumbers below 100 are probably within the inverse cascade region or within the injection region. Ad hoc hyperdiffusion schemes are unlikely to be relevant in those regions. However, the methodology for subgrid scale parameterizations considered in this study is completely general and should be applicable there.

3 Subgrid scale parameterizations

We now seek to reproduce the statistics of the model, obtained at T252, at lower resolutions. To accomplish this, we obtain the subgrid tendency, $(\partial \mathbf{q}(t)/\partial t)_s$, where $\mathbf{q} = (\mathbf{q}_{mn}^1, \mathbf{q}_{mn}^2)^T$, which is the contribution to the right hand side of Equation (1) from non-linear terms such that at least one

of (\mathbf{p}, \mathbf{q}) or (\mathbf{r}, \mathbf{s}) has a wavenumber greater than a specified cutoff wavenumber \mathbf{T}_R ($\mathbf{T}_R < 252$). This subgrid tendency has in general a time independent (mean) part, \mathbf{f}_m , and a time dependent (transient) part, $(\partial \hat{\mathbf{q}}(\mathbf{t})/\partial \mathbf{t})_s$. The latter is not explicitly computed in the LES, but is instead parameterized in terms of resolved scale quantities. In this article, we compare deterministic and stochastic forms of this parameterization. The deterministic parameterization is

$$\left(\frac{\partial \hat{\mathbf{q}}(\mathbf{t})}{\partial \mathbf{t}}\right)_s = -\mathbf{D}_n \hat{\mathbf{q}}(\mathbf{t}), \quad (2)$$

where \mathbf{D}_n is a 2×2 matrix defined as the net dissipation matrix; $\hat{\mathbf{q}} = \mathbf{q} - \bar{\mathbf{q}}$ is the transient part of \mathbf{q} ; and $\bar{\mathbf{q}}$ is the mean part of \mathbf{q} . Multiplying Equation (2) by $\hat{\mathbf{q}}^\dagger(\mathbf{t})$ and averaging, we obtain

$$\mathbf{D}_n = - \left[\left\langle \left(\frac{\partial \hat{\mathbf{q}}(\mathbf{t})}{\partial \mathbf{t}}\right)_s \hat{\mathbf{q}}^\dagger(\mathbf{t}) \right\rangle \right] \left[\langle \hat{\mathbf{q}}(\mathbf{t}) \hat{\mathbf{q}}^\dagger(\mathbf{t}) \rangle \right]^{-1}. \quad (3)$$

Here, angle brackets denote time averaging. The stochastic parameterization is

$$\left(\frac{\partial \hat{\mathbf{q}}(\mathbf{t})}{\partial \mathbf{t}}\right)_s = -\mathbf{D}_d \hat{\mathbf{q}}(\mathbf{t}) + \hat{\mathbf{f}}_b(\mathbf{t}). \quad (4)$$

Here, \mathbf{D}_d is a 2×2 matrix defined as the drain dissipation matrix and $\hat{\mathbf{f}}_b$ is a random forcing (also known as the stochastic backscatter) vector of order two. As shown by Frederiksen and Kepert [5], the drain dissipation matrix is computed by multiplying Equation (4) by $\hat{\mathbf{q}}^\dagger(\mathbf{t}_0)$ (where $\mathbf{t}_0 < \mathbf{t}$), integrating over the time interval $\tau = \mathbf{t} - \mathbf{t}_0$ and averaging. Hence,

$$\mathbf{D}_d = - \left[\int_{\mathbf{t}_0}^{\mathbf{t}} \left\langle \left(\frac{\partial \hat{\mathbf{q}}(s)}{\partial \mathbf{t}}\right)_s \hat{\mathbf{q}}^\dagger(\mathbf{t}_0) \right\rangle ds \right] \left[\int_{\mathbf{t}_0}^{\mathbf{t}} \langle \hat{\mathbf{q}}(s) \hat{\mathbf{q}}^\dagger(\mathbf{t}_0) \rangle ds \right]^{-1}. \quad (5)$$

The noise covariance matrix

$$\mathbf{F}_b = \left\langle \hat{\mathbf{f}}_b(\mathbf{t}) \hat{\mathbf{q}}^\dagger(\mathbf{t}) \right\rangle + \left\langle \hat{\mathbf{q}}(\mathbf{t}) \hat{\mathbf{f}}_b^\dagger(\mathbf{t}) \right\rangle \quad (6)$$

may be obtained from the Lyapunov equation

$$\begin{aligned} \left\langle \left(\frac{\partial \hat{\mathbf{q}}(t)}{\partial t} \right)_s \hat{\mathbf{q}}^\dagger(t) \right\rangle + \left\langle \hat{\mathbf{q}}(t) \left(\frac{\partial \hat{\mathbf{q}}(t)}{\partial t} \right)_s^\dagger \right\rangle \\ = -\mathbf{D}_d \langle \hat{\mathbf{q}}(t) \hat{\mathbf{q}}^\dagger(t) \rangle - \langle \hat{\mathbf{q}}(t) \hat{\mathbf{q}}^\dagger(t) \rangle \mathbf{D}_d^\dagger + \mathbf{F}_b(t) \end{aligned} \quad (7)$$

after computing \mathbf{D}_d . The forcing, $\hat{\mathbf{f}}_b(t)$, is assumed to be white noise and may then be constructed as shown in the dissertation of Zidikheri [6].

4 Model results

Equations (3), (5) and (7) are then used to calculate the matrix parameters \mathbf{D}_n , \mathbf{D}_d , and \mathbf{F}_b . We study subgrid scale parameterizations at T31 using a two stage procedure. Firstly, an LES is constructed at T126, and then this LES is used to calculate the matrix parameters for the T31 LES. The matrix structure of the parameters is simplified when work with the barotropic and baroclinic modes defined in Section 2. It is easy to show that the matrices \mathbf{D}_d and \mathbf{F}_b transform into $\mathcal{D}_d = \mathbf{M} \mathbf{D}_d \mathbf{M}^{-1}$ and $\mathcal{F}_b = \mathbf{M} \mathbf{F}_b \mathbf{M}^\dagger$, where

$$\mathbf{M} = \frac{1}{2} \begin{pmatrix} 1 & 1 \\ \frac{1}{c} & -\frac{1}{c} \end{pmatrix}. \quad (8)$$

Here, $c = 1 + 2F_L[n(n+1)]^{-1}$. Because of the symmetry of the equivalent layer system, it turns out that \mathcal{D}_d and \mathcal{F}_b have purely real diagonal elements and purely imaginary off-diagonal elements.

The matrix parameters are firstly calculated for $T_R = 126$ using a sampling time of 104 days and $\tau = 1$ day. An LES is then performed at T126, and this is run for 2700 days. The parameters \mathcal{D}_n , \mathcal{D}_d , and \mathcal{F}_b were calculated from this simulation with $T_R = 31$; they are shown in Figures 2 and 3 after being averaged over the zonal wavenumber m . Note that the parameters are anisotropic, and the averaging over m is mainly for display

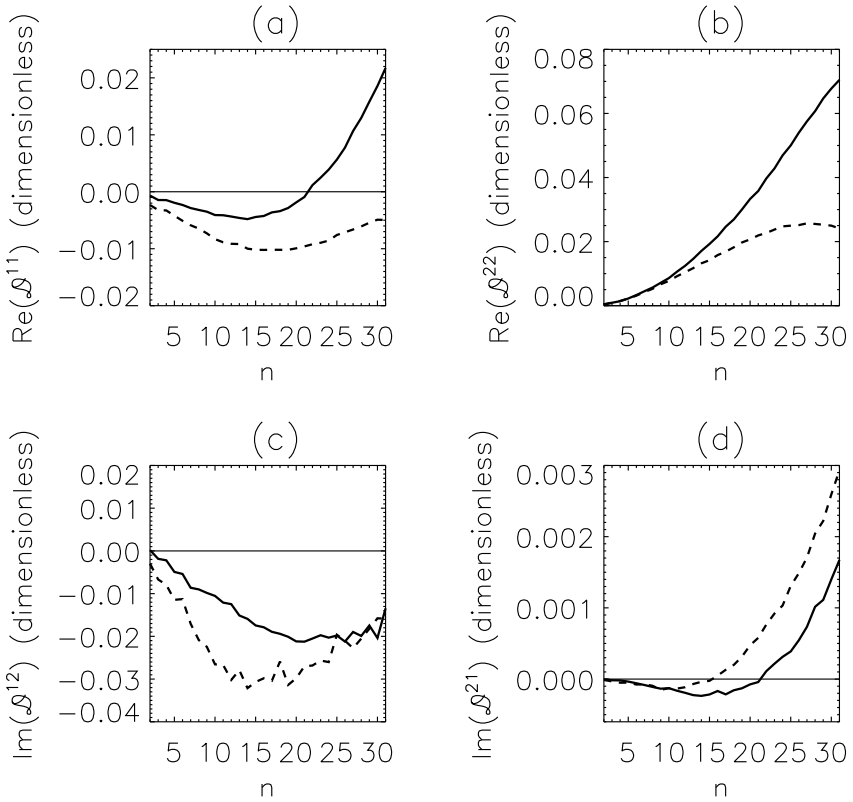


FIGURE 2: Eddy dissipation matrix coefficients: (a) $\Re(\mathcal{D}^{11})$, (b) $\Re(\mathcal{D}^{22})$, (c) $\Im(\mathcal{D}^{12})$, and (d) $\Im(\mathcal{D}^{21})$ as functions of total wavenumber n with $T_R = 31$, with drain dissipation shown in solid lines and net dissipation in dashed lines.

purposes; in the LES, the full \mathbf{m} and \mathbf{n} dependent parameters are used. The net dissipation matrix parameters, $\mathcal{D}_{\mathbf{n}}$, are shown as dashed lines in Figure 2. The ‘barotropic’ diagonal element ($\mathcal{D}_{\mathbf{n}}^{11}$) is negative at all wavenumbers while the ‘baroclinic’ ($\mathcal{D}_{\mathbf{n}}^{22}$) diagonal element is positive at all wavenumbers. This is consistent with the phenomenology of quasi-geostrophic two layer turbulence [4]. The barotropic energy is cascaded towards lower wavenumbers while the baroclinic energy is cascaded towards higher wavenumbers for wavenumbers larger than the deformation scale. The off-diagonal elements of $\mathcal{D}_{\mathbf{n}}$ are also significant; the $\mathcal{D}_{\mathbf{n}}^{12}$ element in particular. The latter is negative at all scales; the $\mathcal{D}_{\mathbf{n}}^{21}$ element is mostly positive. Upon running the LES at T31, we find that the deterministic formulation (employing $\mathbf{D}_{\mathbf{n}}$) is numerically unstable. We hypothesize that the instability is related to the negative values of the diagonal barotropic elements.

For the stochastic parameterization, the matrix parameters $\mathcal{D}_{\mathbf{d}}$ and $\mathcal{F}_{\mathbf{b}}$ were calculated using an integration time, τ , of four days; they are shown as solid lines in Figures 2 and 3. The barotropic diagonal element of $\mathcal{D}_{\mathbf{d}}$ rises to a positive cusp near the truncation scale, and is only slightly negative at low wavenumbers. The baroclinic diagonal element remains positive at all scales, rising to a cusp near the truncation scale. The off-diagonal elements are qualitatively similar to those of $\mathcal{D}_{\mathbf{n}}$, but are changed somewhat in terms of magnitude. The barotropic diagonal element of $\mathcal{F}_{\mathbf{b}}$ rises to a cusp near the truncation scale; it is over an order of magnitude greater than the baroclinic diagonal element. The off-diagonal elements of $\mathcal{F}_{\mathbf{b}}$ are complex conjugates, and are an order of magnitude less than $\mathcal{F}_{\mathbf{b}}^{11}$ (but greater than $\mathcal{F}_{\mathbf{b}}^{22}$). The LES at T31 has been run with $\mathbf{D}_{\mathbf{d}}$ and $\mathbf{F}_{\mathbf{b}}$, and the kinetic energy (Level 1) spectrum is shown in Figure 4. The agreement between the LES at T31 and the higher resolution simulation is excellent.

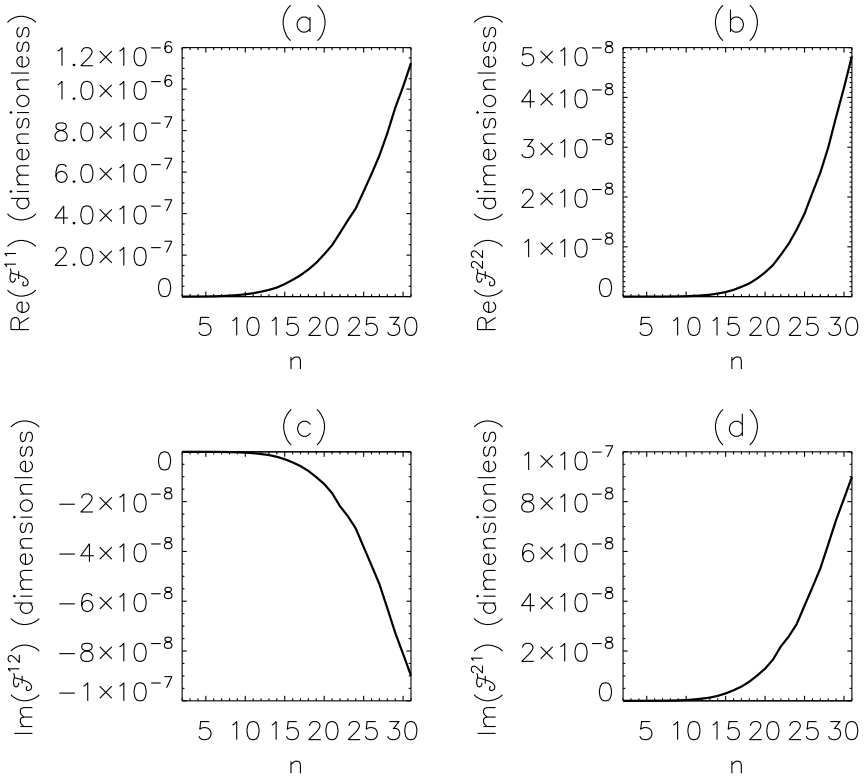


FIGURE 3: Stochastic backscatter covariance matrix coefficients: (a) $\Re(\mathcal{F}^{11})$, (b) $\Re(\mathcal{F}^{22})$, (c) $\text{Im}(\mathcal{F}^{12})$, and (d) $\text{Im}(\mathcal{F}^{21})$ as functions of total wavenumber n with $T_R = 31$.

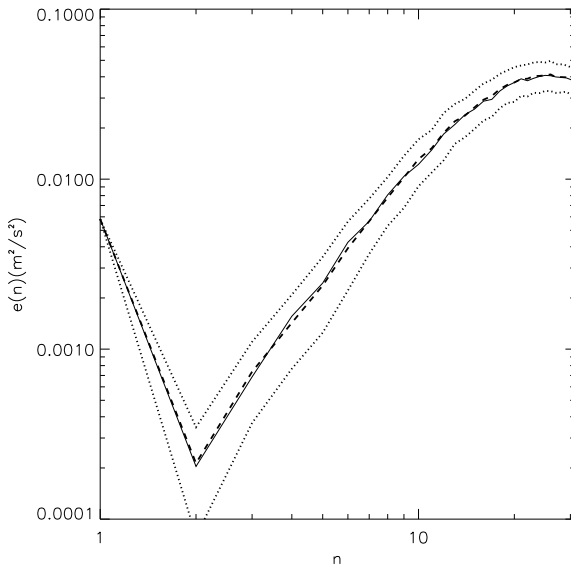


FIGURE 4: Energy spectra as functions of total wavenumber n : kinetic energy for T31 LES (solid); T126 LES kinetic energy truncated back to T31 (dashed); and T31 LES kinetic energy plus and minus standard deviation (dotted).

5 Discussion and Conclusion

We summarize the main result of this study by using a heuristic equation for the barotropic part of the LES:

$$\frac{\partial \mathbf{x}}{\partial t} = \text{resolved terms} - \mathbf{D}\mathbf{x} + \mathbf{f}. \quad (9)$$

Here \mathbf{x} is a resolved barotropic flow mode of wavenumber \mathbf{k} , \mathbf{D} is a scale dependent subgrid eddy dissipation, and \mathbf{f} is a scale dependent subgrid eddy forcing comprising the random forcing and possibly the off-diagonal dissipation term. If $\mathbf{D} < 0$, for some wavenumbers \mathbf{k} , then those amplitudes will tend to grow exponentially. However, the non-linear terms will tend to limit the growth of the instability if there is an adequate sink at the large or small scales. Hence, for example, if \mathbf{D} is sufficiently positive near the truncation scale, then the simulation may well be stable. This is precisely the case for the T31 barotropic drain eddy dissipation calculated in this study. It was found to be slightly negative at the large scales, but had a positive cusp near the truncation scale, and was found to lead to a numerically stable LES. In contrast, we found that if we try to work with the net dissipation and set the random part of \mathbf{f} to zero, then the simulation becomes unstable. It is not hard to see why this might happen. The barotropic net dissipation is negative for all wavenumbers \mathbf{k} in low resolution oceanic simulations; hence, there is not sufficient dissipation in the LES to control the growth caused by the negative dissipation term. In the stochastic formulation, \mathbf{D} has a positive cusp, and furthermore, the white noise forcing has the effect of de-correlating the flow in time, which helps to stabilize the system. The stochastic formulation also has the advantage of simulating the chaotic nature of the interaction between the resolved and subgrid scales in a more realistic fashion.

References

- [1] Leith, C. E., Atmospheric predictability and two-dimensional turbulence, *J. Atmos. Sci.*, **28**, 1971, 145–161.
[doi:10.1175/1520-0469\(1971\)028;0145:APATDT;2.0.CO;2](https://doi.org/10.1175/1520-0469(1971)028;0145:APATDT;2.0.CO;2) C461
- [2] Kraichnan, R. H., Eddy viscosity in two and three dimensions, *J. Atmos. Sci.*, **33**, 1976, 1521–1536.
[doi:10.1175/1520-0469\(1976\)033;1521:EVITAT;2.0.CO;2](https://doi.org/10.1175/1520-0469(1976)033;1521:EVITAT;2.0.CO;2) C461
- [3] Frederiksen, J. S., and A. G. Davies, Eddy viscosity and stochastic backscatter parameterizations on the sphere for atmospheric circulation models, *J. Atmos. Sci.*, **54**, 1997, 2475–2492.
[doi:10.1175/1520-0469\(1997\)054;2475:EVASBP;2.0.CO;2](https://doi.org/10.1175/1520-0469(1997)054;2475:EVASBP;2.0.CO;2) C461, C462
- [4] Salmon, R., Two-layer quasi-geostrophic turbulence in a simple special case, *Geophys. Astrophys. Fluid Dynamics*, **10**, 1978, 25–52.
[doi:10.1080/03091927808242628](https://doi.org/10.1080/03091927808242628) C461, C463, C468
- [5] Frederiksen, J. S. and S. M. Kepert, Dynamical subgrid-scale parameterizations from direct numerical simulations, *J. Atmos. Sci.*, **63**, 2006, 3006–3019. [doi:10.1175/JAS3795.1](https://doi.org/10.1175/JAS3795.1) C462, C463, C465
- [6] Zidikheri, M. J. *Dynamical Subgrid-scale parameterizations for Quasigeostrophic Flows using Direct Numerical Simulations*, PhD Thesis, The Australian National University, 2008. C462, C466
- [7] Bourke, W., An efficient, one-level, primitive-equation spectral model, *Mon. Weath. Rev.*, **100**, 1972, 683–689.
[doi:10.1175/1520-0493\(1972\)100;0683:AEOPSM;2.3.CO;2](https://doi.org/10.1175/1520-0493(1972)100;0683:AEOPSM;2.3.CO;2) C463

Author addresses

1. **Meelis J. Zidikheri**, Department of Theoretical Physics, Research School of Physical Sciences and Engineering, Australian National University, Canberra, AUSTRALIA.
<mailto:meelis.zidikheri@csiro.au>
2. **Jorgen S. Frederiksen**, CSIRO Marine and Atmospheric Research, Aspendale, Victoria, AUSTRALIA.